Virology 424 (2012) 33–44

Contents lists available at SciVerse ScienceDirect

Virology

journal homepage: www.elsevier.com/locate/yviro

HIV-1 Vpu's lipid raft association is dispensable for counteraction of the particle release restriction imposed by CD317/Tetherin

Joëlle V. Fritz, Nadine Tibroni, Oliver T. Keppler, Oliver T. Fackler *

Department of Infectious Diseases, Virology, University of Heidelberg, INF 324, 69120 Heidelberg, Germany

ARTICLE INFO

Article history:
Received 22 September 2011
Returned to author for revision
20 October 2011
Accepted 8 December 2011
Available online 4 January 2012

Keywords:
HIV-1 release
Vpu
CD317
DRM
Lipid rafts
CRAC motif

ABSTRACT

HIV-1 Vpu antagonizes the block to particle release mediated by CD317 (BST-2/HM1.24/Tetherin) *via* incompletely understood mechanisms. Vpu and CD317 partially reside in cholesterol-rich lipid rafts where HIV-1 budding preferentially occurs. Here we find that lipid raft association of ectopically expressed or endogenous CD317 was unaltered upon co-expression with Vpu or following HIV-1 infection. Similarly, Vpu's lipid raft association remained unchanged upon expression of CD317. We identify amino acids V25 and Y29 of Vpu as crucial for microdomain partitioning and single substitution of these amino acids resulted in Vpu variants with markedly reduced or undetectable lipid raft association. These mutations did not affect Vpu's subcellular distribution and binding capacity to CD317, nor its ability to downmodulate cell surface CD317 and promote HIV-1 release from CD317-positive cells. We conclude that (i) lipid raft incorporation is dispensable for Vpu-mediated CD317 antagonism and (ii) Vpu does not antagonize CD317 by extraction from lipid rafts.

Introduction

CD317 (BST-2/Tetherin/HM1.24) is a broadly expressed antiviral restriction factor that impairs the release of enveloped viruses, such as primate lentiviruses, simple retroviruses, filoviruses, arenaviruses, rhabdoviruses and orthomyxoviruses by tethering mature virions to the producer cell-surface (Erikson et al., 2011; Jouvenet et al., 2009; Kaletsky et al., 2009; Mansouri et al., 2009; Neil et al., 2008; Pardieu et al., 2010; Radoshitzky et al., 2010; Sakuma et al., 2009; Van Damme et al., 2008; Weidner et al., 2010; Yondola et al., 2011). By disulfide bonding CD317 forms dimers and it is believed that CD317 connects mature virions and the plasma membrane without the physical involvement of other host cell factors (Hinz et al., 2010; Perez-Caballero et al., 2009; Yang et al., 2010).

To overcome the restriction by CD317, HIV-1 encodes the accessory protein Vpu, which expressed in *cis* or *trans* rescues particle release (Goffinet et al., 2009, 2010; Neil et al., 2008; Tervo et al., 2011; Van Damme et al., 2008). The mechanism by which Vpu antagonizes CD317 remains elusive, even though some insights on how Vpu counteracts CD317 have been described recently. Vpu targets CD317 to proteasomal and/or lysosomal degradation (Goffinet et al., 2009; Gupta et al., 2009; Iwabu et al., 2009; Mangeat et al., 2009; Mitchell et al., 2009), however, depletion of cellular CD317 pools is not essential for Vpu antagonism (Dube et al., 2010; Goffinet et al., 2010; Miyagi et al., 2009; Tervo et al., 2011). Vpu also reduces cell-surface exposure of CD317 (Dube et al., 2010; Goffinet et al., 2010; Mitchell et al., 2009; Van Damme et al., 2008), an effect that correlates in qualitative terms with antagonism of the CD317-imposed virion release restriction. Vpu reduces the cell-surface population of CD317 by inhibiting both the anterograde transport of newly synthesized CD317 and the recycling of CD317 to the cell surface, while the kinetics of CD317 endocytosis remain unaffected (Andrew et al., 2011; Dube et al., 2010; Lau et al., 2011; Mitchell et al., 2009; Schmidt et al., 2011). Moreover, Vpu physically associates with CD317 (Banning et al., 2010; Kobayashi et al., 2011; Mangeat et al., 2009; Rong et al., 2009; Vigan and Neil, 2010), giving rise to the current model that Vpu directly sequesters CD317 away from HIV-1 budding sites at the plasma membrane (PM) to prevent virion tethering during HIV-1 release.

CD317 as well as Vpu partially reside in cholesterol- and sphingolipid-rich membrane microdomains (also referred to as lipid rafts) where HIV-1 budding preferentially occurs (Holm et al., 2003; Kupzig et al., 2003; Lindwasser and Resh, 2002; Masuyama et al., 2009; Nguyen and Hildreth, 2000; Ono and Freed, 2001; Rollason et al., 2007; Ruiz et al., 2010). Lipid rafts are viewed as integration platforms for many factors essential for cellular processes, such as cell signaling and trafficking (Brown and Rose, 1992; Li et al., 2003; Simons and Ikonen, 1997) and are composed of lipid–lipid and lipid–protein interactions (for review: (Lingwood and Simons, 2010)). Lipid rafts

* Corresponding author at: Department of Infectious Diseases, Virology, University of Heidelberg, Im Neuenheimer Feld 324, D-69120 Heidelberg, Germany. Fax: +49 6221 565003.
E-mail addresses: joelle.fritz@med.uni-heidelberg.de (J.V. Fritz), nadine.tibroni@med.uni-heidelberg.de (N. Tibroni), oliver.keppler@med.uni-heidelberg.de (O.T. Keppler), oliver.fackler@med.uni-heidelberg.de (O.T. Fackler).

0042-6822/$ – see front matter © 2011 Elsevier Inc. All rights reserved.
doi:10.1016/j.virol.2011.12.008

are most prominently found at the plasma membrane, but were also described within membranes of the endoplasmatic reticulum (ER), the Golgi apparatus and the endocytic system (Browman et al., 2006; Morrow and Parton, 2005). Due to their insolubility to non-ionic detergents such as Triton X-100 at 4 °C, membrane rafts are often also referred to as detergent-resistant membranes (DRMs). CD317 is targeted to lipid rafts *via* its GPI anchor, which is also essential for its antiviral activity (Kupzig et al., 2003; Neil et al., 2008; Perez-Caballero et al., 2009; Rollason et al., 2007). Interestingly, in CHO cells defective in expression of PIGL, an ER-resident enzyme required for the addition of GPI anchors, CD317 is trapped in the ER and cannot be detected at the PM. Reconstitution of the PIGL defect allows CD317 to reach the PM, indicating that the GPI anchor is not only required to direct CD317 to lipid rafts but also for efficient trafficking of CD317 to the PM where CD317 is able to tether mature HIV-1 viral particles to the cell surface (Perez-Caballero et al., 2009). Since Vpu interferes with the intracellular trafficking of CD317 (Dube et al., 2009, 2010; Schmidt et al., 2011) and partially resides in lipid rafts (Ruiz et al., 2010), it is plausible that Vpu-mediated antagonism of CD317 may involve alterations in the lipid raft association of the restriction factor and/or may depend on the association of Vpu with these specific membrane microdomains.

In support of such a scenario, a recent study reported a correlation between lipid raft association of Vpu and its antagonism of the CD317-mediated HIV-1 release restriction (Ruiz et al., 2010). However, this study did not analyze whether Vpu affects the lipid raft association of CD317. Moreover, VpuW22A, the Vpu mutant described to be absent from lipid rafts and deficient in counteracting CD317 (Ruiz et al., 2010), was shown in another study to be significantly impaired in binding to CD317 (Vigan and Neil, 2010). Since physical interactions between CD317 and Vpu are required for antagonism by Vpu (Gupta et al., 2009; Kobayashi et al., 2011; Rong et al., 2009; Vigan and Neil, 2010), it remains unclear whether VpuW22A is unable to antagonize CD317 because of its lack in lipid raft association or of its poor binding affinity to CD317.

In the current study we tested whether the lipid raft-associated Vpu subpopulation is critically involved in CD317 antagonism and possibly acts by displacing CD317 from such microdomains. We show that Vpu and CD317 partially co-localized with lipid rafts in the Golgi apparatus, however, the extent of lipid raft association of CD317 was not affected upon overexpression of Vpu or by HIV-1 infection. Similarly, CD317 did affect neither the extent of Vpus' association with lipid rafts nor its subcellular localization. Mutagenesis of a putative cholesterol-binding motif in Vpu resulted in Vpu mutants that virtually lacked lipid raft association, but retained the ability to associate with and reduce cell surface exposure of CD317. Importantly, these non-lipid raft-associated Vpu mutants displayed near wild-type activity in antagonism of the CD317 particle release restriction. We conclude that Vpu's association with lipid rafts is dispensable for its role as a CD317 antagonist.

Results

Vpu and CD317 partially reside in detergent resistant membranes and co-expression of both proteins does not influence their partitioning in these membrane microdomains

We first characterized the partitioning of Vpu and CD317 into lipid rafts. For subsequent analysis of effects of Vpu on DRM partitioning of CD317, we sought to circumvent confounding problems in the interpretation of our experiments due to Vpu-induced degradation of CD317 by using a CD317 mutant that carries lysine-to-alanine mutations on positions 18 and 21 (KKAA). CD317 KKAA efficiently restricts the release of HIV-1Δ*vpu* and is readily antagonized by Vpu, but is insensitive to Vpu-induced degradation (Goffinet et al., 2010). To test whether the overall lipid raft association of CD317 KKAA was comparable to that of wild-type (wt) CD317, 293T cells were transfected with an expression plasmid for HA-tagged CD317 and 24 h posttransfection, detergent-resistant membranes (DRMs) were extracted using an established flotation assay following cell lysis in cold Triton X-100 containing buffer and Optiprep gradient ultracentrifugation (Rauch et al., 2008). By using this method we isolated DRMs that were most probably depleted for tetraspanin-enriched membrane microdomains, but contained lipid rafts and caveolae (Zheng and Foster, 2009). Therefore, the term DRM used in this study refers to lipid rafts and caveolae only. Eight 500 µl fractions were collected from the top of the gradient. Since intermediate fractions of these gradients are largely devoid of protein (Krautkramer et al., 2004; Ruiz et al., 2010), equal volumes of fraction 2 (the DRM fraction), fraction 8 (the soluble fraction (S)) and of the total cell lysate (I) were analyzed by Western blotting (Figs. 1A and B). Transferrin receptor (Tfr; excluded from DRMs) and Caveolin (Cav; DRM-resident) served as quality control for the fractionation. As reported before (Goffinet et al., 2010) CD317 wt and KKAA displayed differences between the relative intensity of individual CD317 species. These most likely reflect differential posttranslational modification but their individual occurrence does not have predictive value for the antiviral function of CD317 and for sensitivity to Vpu (Goffinet et al., 2010). While individual protein species displayed differential affinity for the DRM fraction, analyzing the distribution of all species together revealed that the overall distribution of both CD317 variants between DRM and S fractions was comparable (Figs. 1A and B; 31% versus 29% (DRM) and 69% versus 71% (S), respectively; see Methods section for details on Western blot quantification).

To analyze lipid raft association in the absence of detergent we next assessed the co-localization of either CD317 KKAA or Vpu with lipid raft markers by confocal microscopy (Figs. 1C, D and F). PM microdomains were visualized *via* clustering of fluorescently labeled cholera toxin (Ctx) (Giese et al., 2006; Krautkramer et al., 2004) in Jurkat Tag T cells transiently expressing untagged or HA-tagged CD317 variants (Fig. 1C). Surprisingly, only a small population of CD317 wt and KKAA partially co-localized with Ctx cluster at the PM, irrespective of the HA tag. We therefore also investigated the localization to intracellular microdomains in 293T cells using Flotilin-1.GFP as ubiquitous DRM marker which is enriched in the *trans*-Golgi network (TGN) but can also be detected at the PM (Browman et al., 2006) and found that CD317 KKAA (Fig. 1D; upper panels) (and CD317 wt, data not shown) and Flotilin-1.GFP localized to the same perinuclear area. In contrast, little overlap was observed with Erlin-1.GFP, a DRM-resident protein localized at the endoplasmic reticulum (Fig. 1D; lower panels) (Browman et al., 2006). Together, these results suggest that the KKAA mutation has no major effect on CD317's lipid raft association or its overall subcellular localization and suggest that, at least in 293T cells, the majority of CD317 resides in intracellular rather than PM rafts. Analogous DRM association analyses were conducted for Vpu. Consistent with a recent report (Ruiz et al., 2010), approx. 20% of the total cell-associated codon-optimized HIV-1 Vpu_{NL4-3} (Vpu) resided in DRMs (Fig. 1E, see quantification in Fig. 2B, black bars) and intracellular aggregates of Vpu stained positive for Flotilin-1, but not for Erlin-1 in 293T cells (Fig. 1F).

We next tested the hypothesis that Vpu directly sequesters CD317 away from HIV-1 budding sites at the PM by altering the lipid raft association of CD317 and analyzed DRM partitioning of Vpu and CD317 upon co-expression of both proteins. Flotation analysis of transiently transfected 293T cells demonstrated that the relative DRM association of both, Vpu and CD317 KKAA remained largely constant irrespective of whether the two proteins were expressed separately or in combination (Fig. 2A; see also quantification in Fig. 2B (Vpu) and Fig. 2C (CD317 KKAA)). Co-expression also failed to shift Vpu or CD317 to fractions in-between 2 and 8 in our flotation analyses (data not shown). In intact cells, CD317 KKAA was depleted from the cell surface in the presence of Vpu and co-localized with the viral protein as well as with Flotilin-1 in the TGN region (Fig. 2D: upper panels). Only partial co-localization was observed with Erlin-

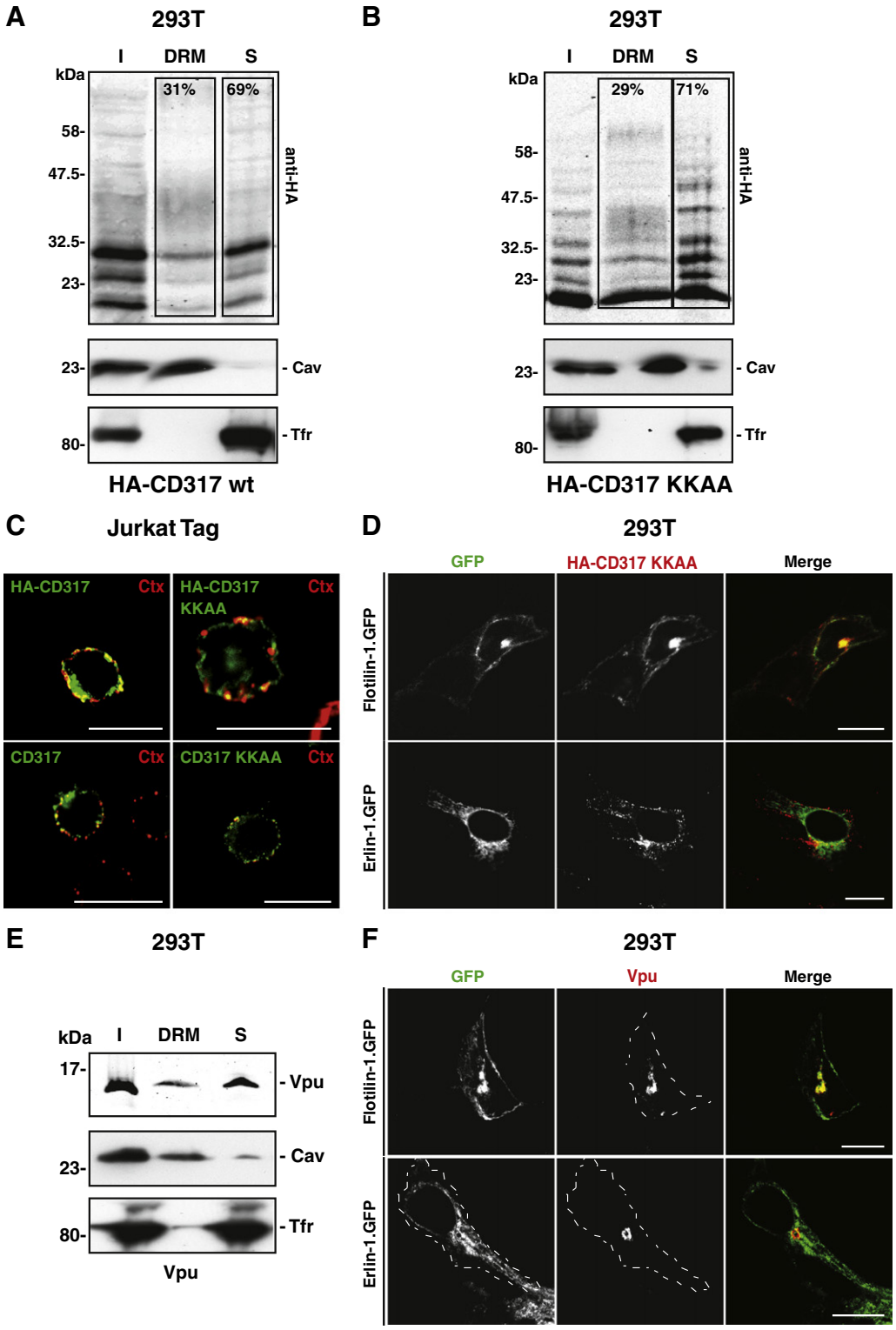

Fig. 1. Vpu and CD317 partially reside in DRMs. (A, B) Western blot (WB) of a detergent resident membrane (DRM) flotation assays of 293T cells transiently expressing HA-CD317 wt (A) or the Vpu depletion resistant mutant HA-CD317 KKAA (B). Cell lysates (cold 1% Triton X-100) were separated by Optiprep gradient ultracentrifugation, and eight fractions were collected from the top (fraction 1) to the bottom (fraction 8) of the gradient. The DRM (fraction 2) and the soluble fraction (S) (fraction 8) were analyzed together with the unfractionated cell lysate (I). For DRM and S, 10% of each fraction was loaded; I corresponds to 5% of the total lysate. Caveolin (Cav) and transferrin receptor (Tfr) are quality controls for DRM and S fractions, respectively. The relative distribution of CD317 between DRM and S fractions was determined by Licor quantification as indicated with the combined total signal in both fractions set to 100%. The quantified areas are highlighted by rectangles. Within these rectangles all the bands were quantified after subtraction of a calculated average background value for a given membrane. All visible bands are specific since no signal could be detected on mock transfected cells with the HA-antibody used to detect the different CD317 variants (data not shown (Goffinet et al., 2010; Tervo et al., 2011)). (C) Micrographs of Jurkat Tag T cells transfected with expression plasmids for the indicated CD317 variants following raft clustering by incubation with Cholera toxin (Ctx) conjugated with Alexa 555 fluorescent dye and subsequently cross-linking with anti-Ctx antibody. Anti-CD317 and appropriate Alexa 488 coupled secondary antibodies were used to stain CD317 in green; Ctx is depicted in red. Scale bars: 10 μm. (D) Micrographs of 293T cells transfected with expression plasmids for HA-CD317 KKAA (red) and Flotilin-1.GFP (green) or Erlin-1.GFP (green). Flotilin-1 and Erlin-1 are exclusively DRM-associated proteins enriched in the plasma membrane and TGN or in the ER, respectively. Scale bars: 10 μm. (E) WB of a DRM flotation assay of 293T cells transiently expressing codon-optimized Vpu (Vpu). (F) Micrographs of 293T cells transfected with expression plasmids for Vpu (red) and Flotilin-1.GFP (green) or Erlin-1.GFP (green). Scale bars: 10 μm.

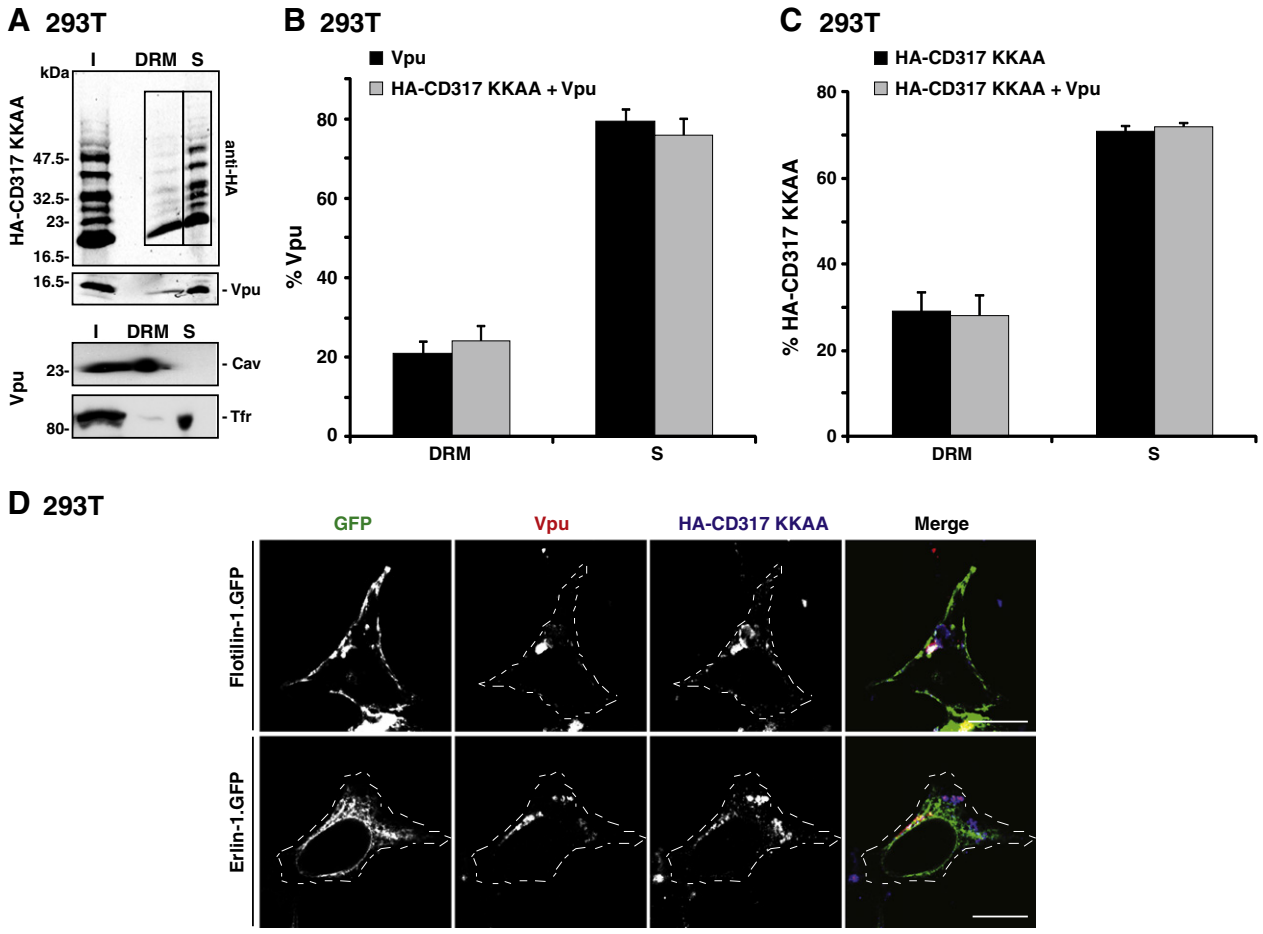

Fig. 2. Co-expression of Vpu and CD317 does not influence the extent of both proteins in DRMs. (A) WB of a representative DRM flotation assay of 293T cells transiently expressing HA-CD317 KKAA and Vpu. The rectangles represent the quantified area (see legend to Fig. 1 for details). (B) Quantification of segregation of Vpu to DRM and S fractions in the absence (black bars) or presence (grey bars) of HA-CD317 KKAA. (C) Quantification of segregation of HA-CD317 KKAA to DRM and S fractions in the absence (black bars) or presence (grey bars) of Vpu. In (B) and (C), the combined total signal of both fractions of the respective protein was set to 100%. Shown are mean values of three independent DRM flotation assays ± SD. (D) Micrographs of 293T cells transfected with expression plasmids for Vpu (red), HA-CD317 KKAA and Flotilin-1.GFP (green) or Erlin-1.GFP (green). Scale bars: 10 μm.

1 in the ER (Fig. 2D: lower panels). Thus, although Vpu and CD317 partially reside in lipid rafts and co-localize at the TGN, Vpu does not affect the overall microdomain association of CD317. This provides evidence that Vpu does not antagonize the particle release restriction of CD317 by extracting the restriction factor from lipid rafts.

A putative CRAC motif in the hinge region of the TM domain and the cytosolic domain of Vpu is important for Vpu's DRM association

Next we wanted to address whether the lipid raft association of Vpu is critical for its role as CD317 antagonist. To this end we sought to define specific lipid raft-targeting motifs in Vpu. A highly conserved motif in the hinge region of Vpu's transmembrane and cytosolic domain was identified (Fig. 3A) reminiscent of a cholesterol recognition amino acid consensus (CRAC) motif that mediates interactions with cholesterol-rich microdomains of e.g. the benzodiazepine receptor (Li and Papadopoulos, 1998) or HIV-1 gp41 (Vishwanathan et al., 2008). A set of Vpu variants with mutations in this putative CRAC motif was generated, Vpu V25G, Vpu Y29G and the double mutant Vpu V25GY29G (Fig. 3B). DRM flotation assays performed with 293T cells transiently expressing Vpu wt or one of the three Vpu mutants demonstrated that each of these CRAC motif mutants displayed strongly reduced DRM association, resulting in an up to 7-fold diminished presence of Vpu in DRMs compared to the wt protein (Fig. 3C, quantification in Fig. 3D).

Functional characterization of putative CRAC motif Vpu mutant

To characterize these Vpu mutants lacking DRM incorporation we first compared their subcellular distribution to that of Vpu wt (Fig. 4A). 293T or Jurkat Tag T cells were transfected with expression constructs for the different Vpu variants and 24 h posttransfection cells were fixed and stained for Vpu. All Vpu mutants showed comparable levels of expression and, independently of the cell type used, displayed a subcellular localization in the perinuclear region (Fig. 4A). This subcellular localization was indistinguishable from that of Vpu wt and thus presumably reflects the localization of Vpu to the TGN (Dube et al., 2009; Hauser et al., 2010; Schmidt et al., 2011; Vigan and Neil, 2010). To further characterize the Vpu CRAC motif mutants, we addressed if they co-localize with endogenous CD317 in TZM-bl cells. Staining for Vpu and CD317 24 h post transfection with expression constructs for the different Vpu variants revealed that Vpu wt as well as all the Vpu mutants showed partial co-localization with CD317 in the perinuclear region (Fig. 4B).

Since the physical interaction between Vpu and CD317 is mediated by the transmembrane domains of both partners and this interaction is essential for Vpu antagonism of CD317 (Gupta et al., 2009; Kobayashi et al., 2011; Rong et al., 2009; Vigan and Neil, 2010), we next determined if Vpu is still able to interact with CD317 when carrying single or double mutations in the putative CRAC motif. 293T cells were transfected with expression constructs for either wt HA-tagged CD317, CD317 KKAA or the Vpu-binding deficient mutant

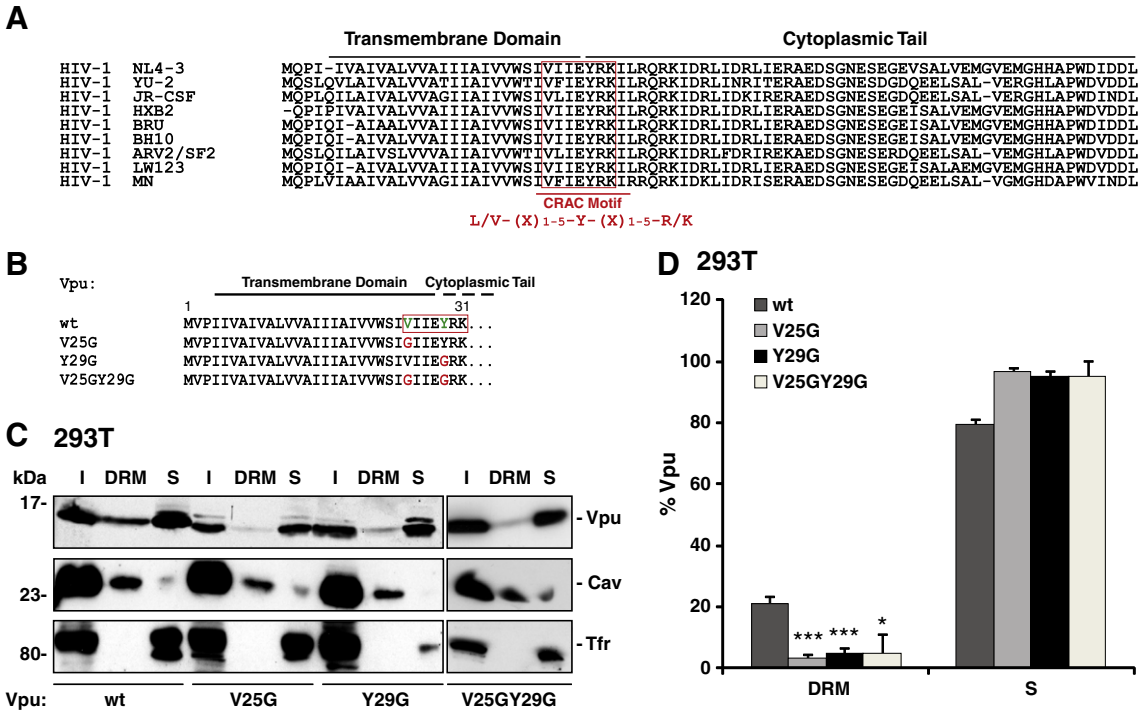

Fig. 3. A putative CRAC motif in the hinge region of the TM domain and the cytosolic domain of Vpu is important for Vpus' DRM association. (A) Alignment of HIV-1 (group M) Vpu amino acid sequences. In red are highlighted the conserved putative cholesterol recognition amino acid consensus (CRAC) motif, the consensus sequence of which is depicted below. (B) Amino acid alignment of Vpu mutants used in this study. (C) WB of a representative DRM flotation assay performed with 293T cells expressing either Vpu wt or the Vpu mutants described in B. (D) Quantification of segregation of Vpu and its mutants into DRM and S fractions in 293T cells. Depicted are arithmetic mean values from three independent DRM flotation assays ± SD. Student's *t*-test: *p<0.05, **p<0.02; ***<0.002.

CD317 T45IΔGI (Kobayashi et al., 2011) and the different Vpu variants. 24 h post transfection cell lysates were immunoprecipitated with an anti-HA antibody and immunoprecipitates (IP) as well as untreated cell lysates (I) were analyzed for the presence of Vpu and CD317 by Western blotting (Fig. 5). As shown in Fig. 5A (left panel) and 5B, all Vpu variants were co-immunoprecipitated with CD317 wt or CD317 KKAA with comparable efficiency. In contrast, none of the Vpu variants was co-immunoprecipitated with CD317 T45IΔGI (Fig. 5C). Since the Vpu mutant W22A was described to be absent from lipid rafts and deficient in counteracting CD317 (Ruiz et al., 2010) we also included this Vpu W22A in our co-immunoprecipitation analysis (Fig. 5A, right panel). In contrast to Vpu wt and the Vpu CRAC motif mutants, binding of VpuW22A to CD317 was significantly reduced but not abolished. In agreement with the report by Vigan and Neil (2010), introduction of a second point mutation, A14L, resulted in the Vpu mutant A14LW22A that was completely deficient in binding to CD317 (Fig. 5A, right panel). We conclude that lipid raft association is not a prerequisite for the physical association of Vpu with CD317 and that the reported defect of Vpu W22A in counteracting CD317 (Ruiz et al., 2010) may reflect its reduced binding affinity to CD317 rather than its lack in lipid raft association.

We next employed the Vpu variants with mutations in the putative CRAC motif to analyze the relevance of Vpu's lipid raft association for its capacity to downregulate surface levels of CD317 and CD4. A3.01 T lymphocytes that endogenously express CD317 and CD4 were electroporated with expression constructs for either Vpu and GFP or an empty vector and GFP. 48 h posttransfection, cells were stained for cell-surface levels of both receptors and analyzed by flow cytometry (Dube et al., 2010; Goffinet et al., 2010; Mitchell et al., 2009; Van Damme et al., 2008). Interestingly, wt as well as mutant Vpu proteins induced a comparable and significant reduction of CD317 cell-surface levels to approximately 60% of those observed in GFP-expressing control cells (Fig. 6A). A similar effect was also seen for endogenous CD317 in HeLa-derived TZM-bl cells (data not shown). In contrast, the integrity of the putative CRAC motif was critical for Vpu-mediated downregulation of cell-surface CD4, with the single and double mutants displaying intermediate or abolished activity, respectively (Fig. 6A). Thus, the putative CRAC motif mediates lipid raft association of Vpu and affects the downregulation of cell surface CD4 (Fig. 6C). In contrast, it is dispensable for Vpu's ability to reduce CD317 cell-surface levels.

We next investigated these Vpu CRAC motif mutants for their ability to rescue virus release in CD317-expressing cells. To this end, 293T cells were co-transfected with HIV-1Δ*vpu* proviral plasmid DNA as well as expression plasmids for HA-CD317 and Vpu. 48 h posttransfection, cell culture supernatants were monitored for levels of released infectious HIV-1 in a TZM-bl reporter cell assay (Keppler et al., 2005). CD317 expression resulted in an approximately 20-fold reduction in the release of infectious HIV-1Δ*vpu* (Fig. 6B). When provided in *trans*, Vpu wt, as well as Vpu V25G and Vpu Y29G, enhanced HIV-1 release approximately 10-fold (Figs. 6B and C). Since the Vpu variants were virtually absent from lipid rafts, this result indicates that lipid raft association is not a prerequisite for antagonism of CD317. In contrast, HIV-1 release by the double CRAC motif mutant was significantly reduced (Figs. 6B and C), suggesting that this Vpu mutant is defective in parameters in addition to lipid raft association. Concordant Western blot analyses of lysates of the virus-producing cells confirmed similar expression of all Vpu variants tested (Fig. 6B, lower panel). Consistent with previous observations and for reasons currently unknown (Serra-Moreno et al., 2011), cell-associated levels of p55 Gag and p24CA were diminished upon CD317 overexpression. However, cell-associated Gag levels were constant in all samples with CD317 overexpression whether or not Vpu was co-expressed, allowing us to compare the efficiency of HIV-1 release between these samples. Cellular CD317 levels were decreased

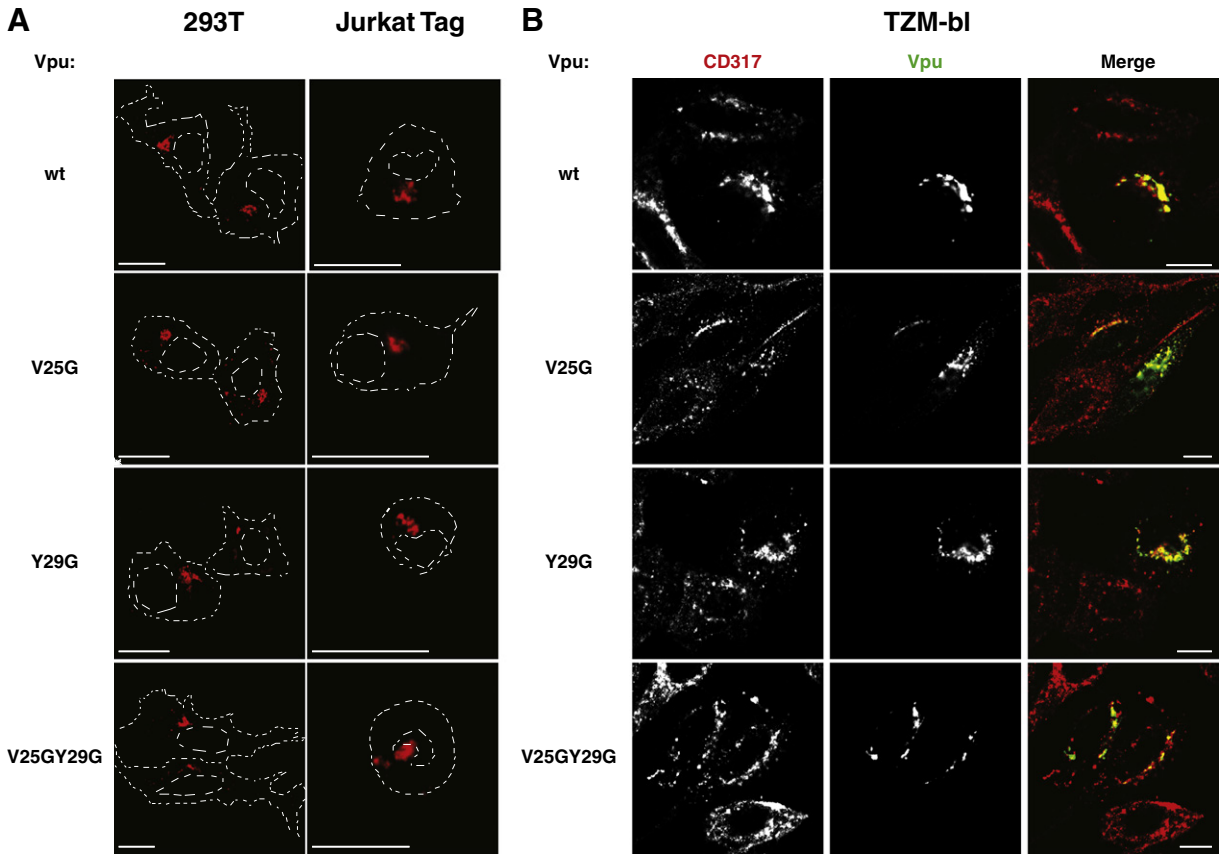

Fig. 4. Vpu wt and CRAC motif Vpu mutants display equal cellular distribution and co-localization with CD317. (A) Micrographs of 293T cells (left column) and Jurkat Tag T cells (right column) transfected with expression plasmids for Vpu wt, Vpu V25G, Vpu Y29G, or Vpu V25GY29G. The cell peripheries as well as the nuclei are highlighted by white dashed lines. Scale bars: 10 μm. (B) Micrographs of TZM cells transfected with expression plasmids for Vpu wt, VpuV25G, Vpu Y29G or VpuV25GY29G. 24 h posttransfection the cells were stained for endogenous CD317 (red) and Vpu (green) using the appropriate antibodies. Scale bars: 10 μm.

by co-expression of Vpu wt and all three Vpu mutants, albeit to variable degrees (Fig. 6B, lower panel). Thus, the degree of CD317 degradation under these experimental conditions did not correlate with the viral release enhancement activity of the Vpu variants tested. Based on the results with Vpu variants carrying single mutations in the putative CRAC motif we conclude that lipid raft association of the viral protein can be dispensable for Vpu-mediated antagonism of CD317 particle release restriction.

Characterization of Vpu CRAC motif mutants in the context of HIV-1 infection

We next sought to study the impact of these Vpu CRAC motif mutants in the context of HIV-1 infection and in presence of endogenous CD317. To this end, the *vpu* variants were introduced into the HIV-1_{NL4-3} proviral backbone, and TZM-bl cells, expressing endogenous CD317, were infected with the corresponding viruses. Similar to our results upon ectopic expression of Vpu, DRM flotation of these infected cells 48 h postinfection revealed a markedly reduced DRM association of Vpu V25G relative to Vpu wt (Fig. 7A and quantification in Fig. 7B). Virtually no DRM association was detected for Vpu Y29G and Vpu V25GY29G under these experimental conditions (Figs. 7A and B). Multiple and difficult to resolve bands were detected for endogenous CD317 in these TZM-bl cells. All these species of endogenous CD317 were generally more enriched in DRMs than ectopically expressed HA-tagged CD317 (compare Figs. 2C and 7C, 29% versus 65% DRM association, respectively). Nevertheless and consistent with our previous results with ectopically expressed CD317, wt or mutant Vpu did not significantly affect the DRM association of endogenous CD317 (Fig. 7A, quantification in Fig. 7C).

We next explored the ability of these provirally encoded Vpu CRAC motif mutants to antagonize the CD317-mediated particle release restriction. Virions were produced in the presence of endogenous CD317 by transfection of the different proviral constructs into TZM-bl cells and production of infectious HIV-1 was quantified by titrating the cell supernatant 48 h posttransfection (Fig. 7D). Western blotting of lysates of the virus-producing cells documented comparable cell-associated levels of Vpu and p24CA (Fig. 7D). Endogenously expressed CD317 significantly decreased (18×) the release of HIV-1Δ*vpu* compared to HIV-1wt (Fig. 7D). Despite their reduced or fully abrogated association with DRMs, Vpu V25G and Vpu Y29G retained almost full or complete CD317 antagonizing activity, respectively, confirming in the context of HIV-1 infection that DRM association of Vpu is not a prerequisite for CD317 antagonism. In contrast, HIV-1Vpu V25GY29G, which lacks DRM association but also bears additional defects, was almost as sensitive to the CD317 restriction as HIV-1Δ*vpu* (9× less virus production relative to wt). This reduced antagonism was particularly surprising since Vpu V25GY29G downregulated CD317 cell-surface levels as efficiently as Vpu wt (Fig. 6A). In order to test whether this effect on HIV-1Vpu V25GY29G particle release depends on CD317, we produced viral particles in 293T cells lacking endogenous CD317. As shown in Fig. 7E, all HIV-1 variants released equal amounts of infectious viral particles in absence of CD317 irrespective of their Vpu status and produced comparable levels of cell-associated Vpu and p24CA. These results demonstrate that DRM association is dispensable for the antagonism of the release restriction imposed on HIV-1 release by endogenous CD317. They furthermore

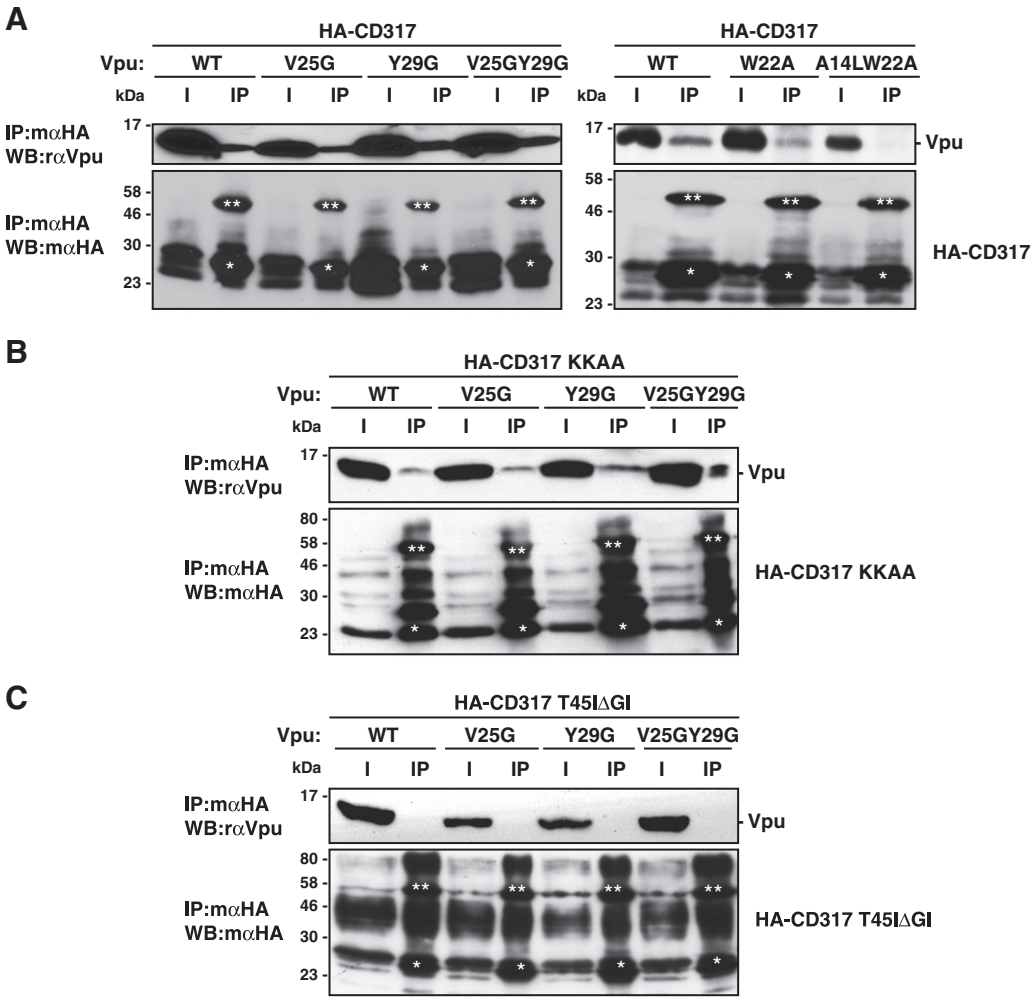

Fig. 5. Association of CRAC motif Vpu mutants with CD317. 293T cells were co-transfected with expression constructs for Vpu wt or the indicated Vpu mutants together with wt HA-tagged CD317 (A), the Vpu depletion resistant mutant HA-CD317 KKAA (B) or with the Vpu binding deficient mutant HA-CD317 T45IΔGI (C), respectively. 24 h later, the different CD317 variants were immunoprecipitated (IP) *via* their HA tag from cell lysates and 10% of the lysates (Input: I) and 75% of the immunoprecipitates were subjected to SDS-PAGE and Western blotting. The light and heavy chains of the HA-antibody used for immunoprecipitation are represented by single and double stars, respectively. The blots shown are representative of at least three independent experiments.

provide an example for the lack of CD317 antagonism in the presence of an overall downregulation of the restriction factor from the surface of virus producing cells.

Discussion

Building on reports on the association of CD317 and Vpu with lipid rafts and the requirement of CD317's lipid raft targeting GPI anchor for its antiviral activity (Kupzig et al., 2003; Perez-Caballero et al., 2009; Rollason et al., 2007; Ruiz et al., 2010), the aim of this study was to test whether incorporation of Vpu into lipid rafts is critically involved in CD317 antagonism. As judged by DRM flotation and confocal microscopy, lipid raft association of either ectopically expressed or endogenous CD317 remained quantitatively unaltered by Vpu in the context of ectopic expression or HIV-1 infection. Moreover, mutation of a putative CRAC motif in Vpu resulted in variants of the viral protein that were virtually absent from lipid rafts while retaining full binding capacity to the restriction factor. These non-microdomain-associated Vpu's downmodulated cell-surface CD317 levels and antagonized the CD317-mediated block to HIV-1 particle release with efficiencies comparable to that of Vpu wt. We conclude that (i) Vpu antagonism of CD317 does not extract the restriction factor from lipid rafts and (ii) lipid raft association is dispensable for its role as a CD317 antagonist.

Our results confirm and expand the previous detection of fractions of cellular pools of Vpu and CD317 in lipid rafts (Kupzig et al., 2003; Rollason et al., 2007; Ruiz et al., 2010). Surprisingly, only a small population of CD317 partially co-localized with Ctx cluster at the PM and Vpu was virtually absent from PM rafts, indicating that the majority of lipid raft association of both proteins results from incorporation into microdomains of intracellular vesicles/membranes. Even though the small size of lipid rafts (10–200 nm), the resolution limits of confocal microscopy and the lack of specific clustering protocols precluded a reliable assessment of protein association with specific microdomains at intracellular membranes, our co-localization studies with Flotilin-1.GFP as ubiquitous DRM marker which is enriched in the TGN (Browman et al., 2006) are consistent with lipid raft partitioning of both Vpu and CD317 at the level of the TGN. While raft-targeting of CD317 is presumably determined by its GPI anchor (Kupzig et al., 2003), we report here that a highly conserved putative CRAC motif embedded in the hinge region of the transmembrane domain and the cytosolic domain of Vpu is required for its lipid raft incorporation. This propensity may reflect a potential interaction of the CRAC motif with cholesterol but, based on the reduced raft targeting of Vpu variants with mutations at additional transmembrane residues (Ruiz et al., 2010), could also mirror “raftophilic” properties of the entire transmembrane domain. A more detailed characterization of the nature of these microdomains and the specific targeting mechanisms

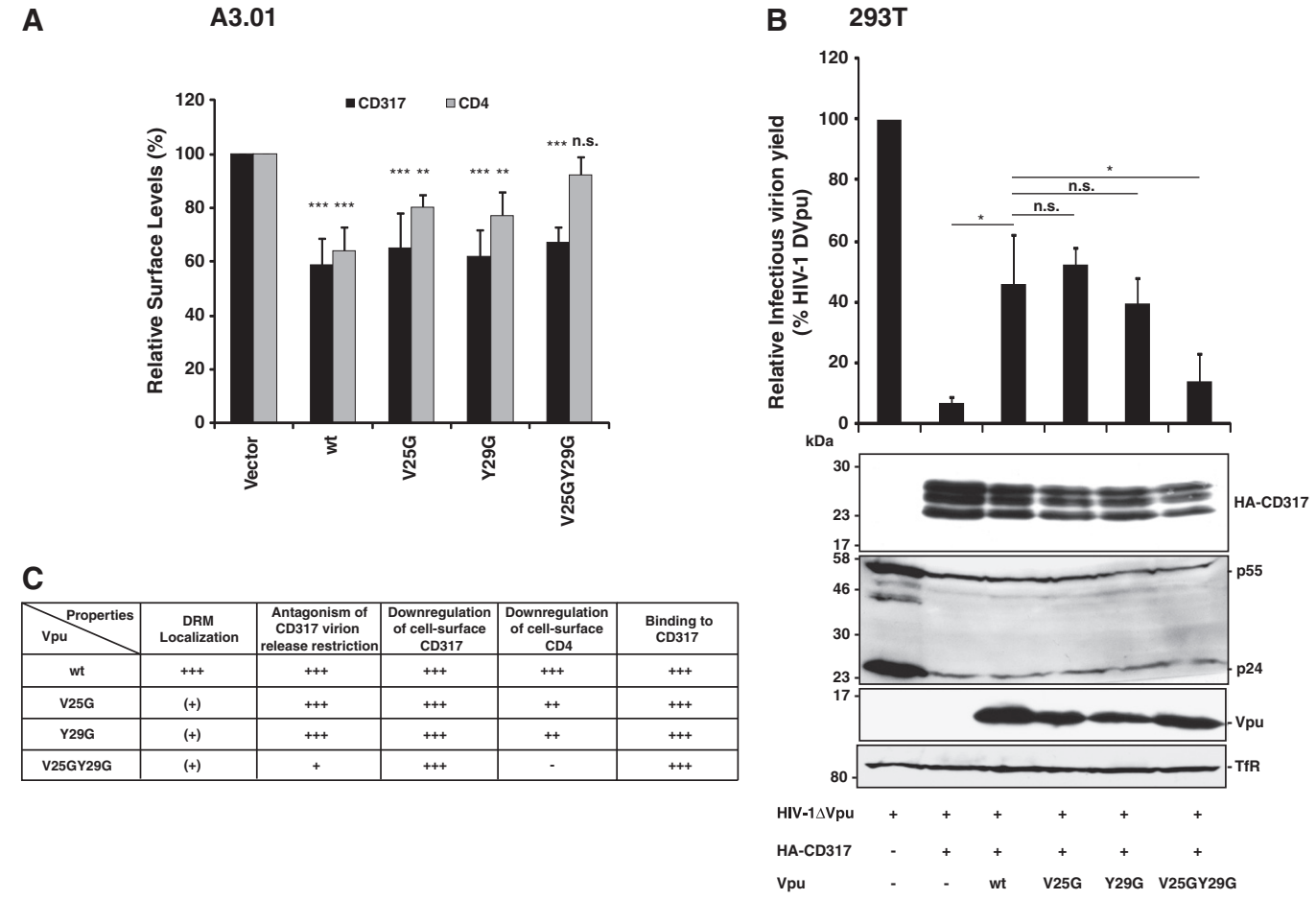

C

Properties / Vpu	DRM Localization	Antagonism of CD317 virion release restriction	Downregulation of cell-surface CD317	Downregulation of cell-surface CD4	Binding to CD317
wt	+++	+++	+++	+++	+++
V25G	(+)	+++	+++	++	+++
Y29G	(+)	+++	+++	++	+++
V25GY29G	(+)	+	+++	-	+++

Fig. 6. CRAC motif Vpu mutants efficiently downregulate cell-surface CD317 and rescue the HIV-1 particle release block imposed by CD317. (A) Relative CD317 and CD4 cell-surface expression levels in A3.01 T cells with values for control cells transfected with the empty vector set to 100%. Arithmetic mean values from three independent experiments ± SD are presented. Statistical significance relative to the empty vector control was assessed by Student's *t*-test (*$p<0.05$, **$p<0.02$; ***<0.002). (B) Upper panel: production of infectious HIV-1 from 293T cells transfected with HIV-1Δ*vpu* proviral DNA and the indicated Vpu and CD317 expression constructs as determined by single-round infectivity assay on TZM-bl reporter cells. Values are given relative to HIV-1Δ*vpu* in the absence of CD317 and represent arithmetic means ± SD of three independent experiments performed in triplicates. Statistical significance relative to Vpu wt was assessed by Student's *t*-test (*$p<0.05$, **$p<0.02$; ***<0.002). Lower panel: Western blot analysis of corresponding 293T cell lysates. (C): Summary of the activity and DRM association of the Vpu variants tested in this study relative to Vpu wt (−: 0–10%; (+): 10–20%; +: 20–33%; ++: 34–66%; +++: 67–100%).

will be an interesting goal of future studies that will require more refined biochemical approaches beyond the Triton-X 100 based extraction protocol used herein.

Mutating two individual amino acids of the putative CRAC motif of Vpu gave rise to the Vpu variants V25G or Y29G that displayed markedly reduced DRM association or were virtually absent from DRM, respectively, when expressed ectopically or from the HIV-1 provirus. Importantly, both Vpu mutants efficiently associated with CD317 and downregulated cell-surface levels of CD317, allowing us to test specifically the relevance of lipid raft association of Vpu for antagonism of CD317. Since both Vpu variants potently overcame the particle release restriction of ectopically expressed and endogenous CD317 with efficiencies that were comparable to that of Vpu wt, lipid raft association of Vpu is clearly not a prerequisite for CD317 antagonism. In light of these results it was surprising that simultaneous mutation of both valine and tyrosine residues (Vpu V25GY29G) resulted in the loss-of-function of Vpu with regard to antagonism of CD317. Since Vpu V25GY29G retains CD317 downregulation and binding activity and the loss of DRM association alone cannot account for its reduced CD317 antagonism, this mutant likely carries additional defects in activities that have not yet been appreciated to be involved in CD317 antagonism. Since Vpu V25GY29G failed to reduce cell surface levels of CD4 and high levels of CD4 can interfere with HIV-1 budding through enforced interactions between CD4 and the viral envelope protein (Ross et al., 1999), this inability to downregulate cell-surface CD4 may be involved in the observed reduction in HIV-1 release from $CD4^+/CD317^+$ cells.

Taken together, the findings presented have implications for our understanding of the mechanism underlying the antagonism of CD317 by Vpu. Our current view of the antagonism mechanism can be integrated into a model in which Vpu, by physical recruitment of the restriction factor (Banning et al., 2010; Kobayashi et al., 2011; Rong et al., 2009; Vigan and Neil, 2010), alters the intracellular transport of newly synthesized and previously internalized pools of CD317 (Andrew et al., 2011; Dube et al., 2009, 2010; Schmidt et al., 2011) at the levels of the TGN to reduce cell surface exposure of CD317 and thus the restriction to particle release (Dube et al., 2010; Goffinet et al., 2009, 2010; Iwabu et al., 2009; Masuyama et al., 2009; Rong et al., 2009; Schmidt et al., 2011; Van Damme et al., 2008; Vigan and Neil, 2010). Within this scenario we hypothesized that these interactions occur in TGN-associated lipid raft microdomains and possibly involve quantitative alterations in lipid raft association. Our results that the overall lipid raft association of CD317 is unaffected by Vpu and that CD317–Vpu interactions do not depend on lipid raft incorporation of the viral protein refute this hypothesis, at least for microdomains isolated by the flotation approach used. In addition, it appears that significantly larger portions of CD317 than of Vpu reside in lipid rafts. The antagonistic activity of Vpu is thus most likely mediated by

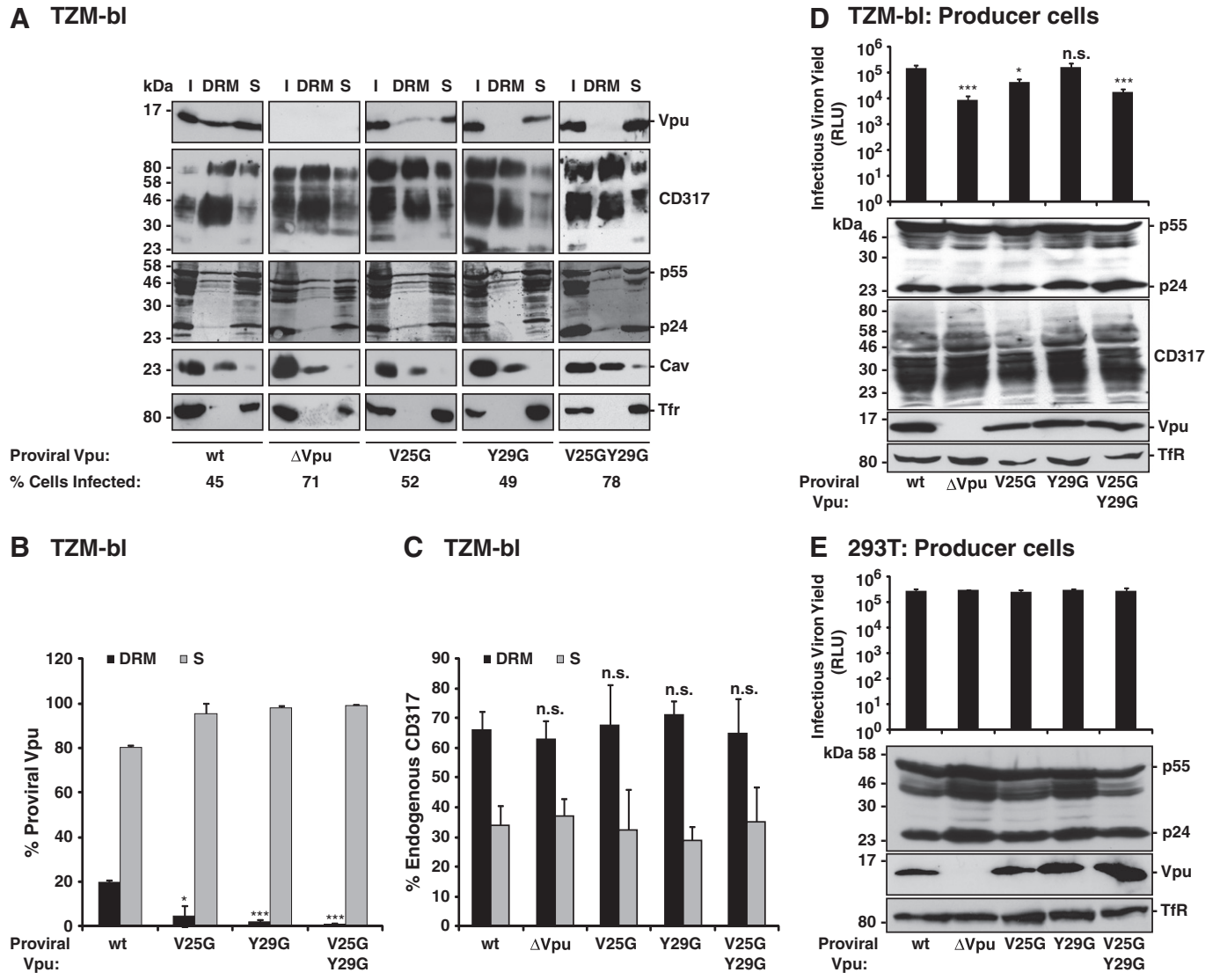

Fig. 7. Characterization of Vpu CRAC motif mutants in the context of HIV-1 infection. (A) Western blot of a representative DRM flotation assay performed with TZM-bl cells infected 48 h prior to the flotation assay with HIV-1 wt, HIV-1Δ*vpu*, or HIV-1 variants encoding the indicated Vpu mutants. A fraction of the infected TZM-bl cells was subjected to quantification of productively infected cells by flow cytometry; the frequency of infected cells is depicted in the bottom line. (B, C) Quantification of segregation of Vpu (B) or endogenous CD317 (C) in DRM and S fractions. For the CD317 blots, all visible bands were quantified. Values depict the mean of three independent DRM flotation assays ± SD. Statistical significance relative to Vpu wt was assessed by paired Student's *t*-test (*$p<0.05$, **$p<0.02$; ***<0.002). (D) TZM-bl cells, expressing endogenous CD317, were transfected with either HIV-1 wt or HIV-1 variants encoding the indicated Vpu mutants. Upper panel: culture supernatants were analyzed for the yield of infectious HIV-1 two days post-infection by single-round infectivity assay on TZM-bl reporter cells. Infectious virion yields are given in relative light units (RLU). Values are arithmetic means ± SD of three independent experiments performed in triplicates. Statistical significance relative to proviral encoded Vpu wt was assessed by paired Student's *t*-test (*$p<0.05$, ***<0.002). Lower panel: representative Western blot analyses from one out of three performed experiments of corresponding TZM-bl cell lysates. (E) 293T cells, lacking endogenous CD317 expression, were transfected with either HIV-1 wt or HIV-1 variants encoding the indicated Vpu mutants. Upper panel: culture supernatants were analyzed for the yield of infectious HIV-1 two days post-infection by single-round infectivity assay on TZM-bl reporter cells. Infectious virion yields are given in RLU. Values are arithmetic means ± SD of three independent experiments performed in triplicates. Lower panel: representative Western blot from one out of three performed experiments of corresponding 293T cell lysates.

non-lipid raft-associated pools of the viral protein. Based on the observation that the physical interaction between Vpu and CD317 is critical for Vpu antagonism, this implies that non-lipid raft-associated Vpu can interact with lipid raft-resident CD317. Based on the lack of altered DRM partitioning of both proteins upon co-expression and the relatively low efficiency of Vpu–CD317 interactions as detected by co-immunoprecipitation in steady state, Vpu–CD317 interactions are likely to be transient. We therefore propose that transient interactions of Vpu with CD317 at the level of the TGN result in alterations of CD317's biological properties that, by a yet to be defined mechanism, reduce its antiviral activity even after the dissociation from Vpu. Importantly, many reports suggest a strong correlation between the downregulation of cell-surface CD317 and Vpu-mediated CD317 counteraction (Dube et al., 2010; Goffinet et al., 2009, 2010; Iwabu et al., 2009; Masuyama et al., 2009; Rong et al., 2009; Schmidt et al., 2011; Van Damme et al., 2008; Vigan and Neil, 2010), implying that reduced transport of CD317 is the major effect of Vpu counteraction. However, Vpu V25GY29G only moderately rescued the CD317-mediated viral release block despite its marked ability to downregulate CD317 cell-surface levels, demonstrating that downregulation of cell-surface CD317 by itself is not fully sufficient for antagonism of the restriction factor. This is in line with two recent studies that described a lack of correlation between CD317 downregulation and Vpu antagonism in certain cell systems (Kuhl et al., 2011; Miyagi et al., 2009). This suggests that so far unknown qualitative changes introduced to CD317 by Vpu at the TGN can disrupt the antiviral activity of the restriction factor. With alterations in both, intracellular transport and biological

activity, CD317 antagonism by Vpu would thus involve two independent mechanisms.

In conclusion, this study provides several lines of evidence that challenge the hypothesis that lipid raft association of Vpu is critical for its antagonism of CD317-mediated restriction to HIV-1 release and rather supports a model in which Vpu's lipid raft association is dispensable for its role as a CD317 antagonist.

Methods

Cells, plasmids, and reagents

Jurkat Tag (JTag) and A3.01 T cells were cultivated in RPMI 1640 supplemented with 10% fetal calf serum, 1% L-glutamine, and 1% penicillin–streptomycin (all from Invitrogen). 293T and TZM-bl cells were maintained in DMEM supplemented with the identical reagents as described for RPMI medium. Proviral plasmids pHIV-1NL4-3 wt (BH10 Env) and pHIV-1NL4-3Δvpu (BH10 Env) were from Valerie Bosch (Pfeiffer et al., 2006). pcDNA-Vphu, expressing a codon-optimized, Rev-independent HIV-1NL4-3 Vpu protein (Nguyen et al., 2004) was from Klaus Strebel. The proviral plasmids pHIV-1NL4-3 Vpu V25G, Vpu Y29G, Vpu V25GY29G, Vpu W22A, and Vpu A14LW22A, as well as the analogous expression constructs for codon-optimized Vpu, were generated by site-directed mutagenesis. Expression constructs for Erlin-1.GFP and Flotilin-1.GFP were kindly provided by Stephen Robbins. N-terminally HA-tagged CD317 wt and CD317 KKAA were described elsewhere (Goffinet et al., 2010). HA-tagged CD317 T45IΔGI was created by site-directed mutagenesis by replacing threonine on position 45 by an isoleucine and deleting glycine and isoleucine on positions 25 and 26.

The following antibodies were used: polyclonal mouse anti-cholera toxin (anti-CTx) (Sigma Aldrich); monoclonal mouse anti-transferrin receptor (Tfr) (clone H68.4) (Zymed Laboratories, Inc.); allophycocyanin (APC)-conjugated mouse-anti human CD4 antibody (clone RPA-T4; BD Bioscience); mouse anti- HM1.24/CD317 (Ishikawa et al., 1995) (5 μg/ml; Chugai Pharmaceutical); rabbit polyclonal anti-BST2/CD317 (kindly provided by Klaus Strebel); rabbit polyclonal anti-Vpu (Biozol), monoclonal mouse anti-HA mAb HA.11 (Covance), polyclonal rabbit anti-Caveolin (Cav) (BD Bioscience); and sheep anti-HIV-1 p24CA antiserum (from Barbara Müller). Secondary fluorescent antibodies and Alexa Fluor 555-conjugated CTx subunit B were obtained from Molecular Probes or BD Bioscience, and protease inhibitor cocktail was purchased from Sigma Aldrich.

Virion infectivity assays

293T cells (1.2×10^5/well) or TZM-bl cells (1×10^5/well) were seeded in 12-well plates 1 day before calcium-phosphate or lipofectamine (Invitrogen) transfection, respectively, of either proviral DNA (1.2 μg, wt or Vpu-mutated variants) alone (Figs. 6D and E) or together with pcDNA3.1-HA-CD317*neo* (0.1 μg) and the indicated Vpu expression constructs (0.12 μg) (Fig. 5B). Two days post-transfection 25 μl of the culture supernatants were added on TZM-bl reporter cells cultured in 96-well and the infectivity of HIV-1 was determined 48 h after infection by analysis of *firefly* luciferase activity (Keppler et al., 2005).

Surface-exposed receptor levels

To quantify CD4 cell surface expression, A3.01 T cells were electroporated with 18 μg of Vpu expression constructs and 2 μg of peGFP, and 48 h post-transfection the cells were washed and stained in PBS with allophycocyanin (APC)-conjugated mouse–anti human CD4 antibodies (clone RPA-T4; BD Bioscience). To quantify CD317 surface-exposure, transfected TZM-bl (0.1 μg of Vpu plasmids and 0.1 μg of peGFP) or A3.01 T cells (18 μg of Vpu plasmids and 2 μg of peGFP) were stained 48 h posttransfection with mouse anti-HM1.24/CD317 (Ishikawa et al., 1995) (5 μg/ml; Chugai Pharmaceutical, Kanagawa, Japan) followed by staining with goat anti-mouse (Alexa Fluor 660) (Invitrogen). A FACSCalibur with BD CellQuest Pro 4.0.2 Software (BD Pharmingen) was used for analysis. The MFI for surface-exposed receptors was quantified in principle as reported (Michel et al., 2005). Relative CD317 and CD4 cell-surface expression levels were normalized to the values obtained for control cells transfected with the empty vector (set to 100%).

Isolation of detergent resistant membranes (DRMs)

Detergent-resistant membranes (DRMs) were isolated by flotation experiments as described previously (Krautkramer et al., 2004). Briefly, 293T cells were transfected with expression constructs for codon-optimized Vpu wt (1.8 μg) and HA-CD317 KKAA (1.5 μg) or for Vpu wt or Vpu variants (1.8 μg) alone using metafectene (Biontex) and incubated for 24 h. A total of 10^6 cells were transfected for each sample. Cells were lysed in 500 μl TXNE buffer (1% Triton X-100, 50 mM Tris HCl [pH 7.4], 150 mM NaCl, and 5 mM EDTA) for 20 min on ice, homogenized with a Dounce homogenizer, and loaded on an Optiprep (Life Technologies) gradient (lysates were adjusted to 40% Optiprep and overlaid with 2.5 ml 28% Optiprep and 600 μl TXNE), followed by ultracentrifugation (35 000 rpm, 3 h, 4 °C). Eight fractions of 500 μl each were collected from the top. Fraction 2, which represented the DRM fraction, and fraction 8, which was indicative of the soluble fraction, was used for Western blot analysis. The quality of the flotation was addressed by using Tfr (excluded from DRMs) and Cav (incorporated in DRMs). For the DRM flotation assay carried out in TZM-bl cells, a million cells were infected with 0.8 μg of VSV-G HIV-1NL4-3 wt (BH10 Env) or Vpu-mutant viruses and 48 h post-infection the DRMs were isolated as described previously.

Cholera toxin clustering

CTx-positive clusters were generated as described before (Krautkramer et al., 2004). A total of 10^7 JTag cells were transfected by electroporation with expression plasmids for HA-tagged or untagged CD317 variants (30 μg). 48 h post-transfection, cells were incubated with 25 μg of Alexa 555-conjugated CTx/ml in 0.1% bovine serum albumin-phosphate-buffered saline for 30 min at 4 °C, followed by addition of anti-CTx antibody (30 min at 4 °C and 10 min at 37 °C). Cells were bound to poly-L-lysine-coated coverslips (5 min, RT), fixed with 3% paraformaldehyde (10 min, RT), and extracted with 0.1% Triton X-100 (1 min, RT). Cells were stained using monoclonal mouse anti-CD317 (Chugai Pharmaceutics), followed by Alexa 488-conjugated secondary antibody, and were mounted in mowiol (Sigma Aldrich). Samples were analyzed by confocal laser scanning microscopy (LSM 510; Zeiss) using a 100× oil immersion objective lens.

Co-precipitation assay

For co-immunoprecipitation analysis, 293T cells (3.6×10^5/6well) transiently expressing Vpu wt or Vpu variants together with HA-tagged CD317, CD317 KKAA or CD317 T45IΔGI, respectively, were harvested 24 h post-transfection and lysed on ice for 30 min in a buffer containing 50 mM Tris–HCl [pH 7.4], 150 mM NaCl, 5 mM EDTA, 1% Triton X-100, and protease inhibitor cocktail (Sigma) before clarification at 4000 ×*g* for 6 min at 4 °C. Ten percent of each lysate was preserved to control for protein expression. The remaining of the cell lysates was incubated for with mouse anti-HA antibody (Covance) (1 h, 4 °C), prior to incubation overnight at 4 °C with pre-cleared protein G sepharose beads. Immunoprecipitates were analyzed for the presence of Vpu and CD317 by Western blotting.

Western blotting

Washed cell pellets were lysed in SDS-lysis buffer. Proteins were separated on 12.5% SDS-PAGE and blotted to nitrocellulose membranes. Blocked membranes were probed with the following primary antibodies: sheep anti-HIV-1 p24CA antiserum (from Barbara Müller), rabbit polyclonal anti-Vpu (Biozol), mouse anti-HA mAb HA.11 (Covance), monoclonal mouse anti-transferrin receptor (Tfr) (clone H68.4) (Zymed Laboratories, Inc.), rabbit polyclonal anti-Bst2/CD317 (provided by Klaus Strebel) and rabbit polyclonal anti Cav (BD Bioscience). Secondary antibodies were conjugated to horseradish peroxidase for ECL-based detection. For detection of proteins with the Licor system (Odyssey® Infrared Imaging System, Biosciences), HRP-conjugated secondary antibodies were replaced with antibodies labeled with IRDye infrared dyes.

Western blotting quantification

The relative distribution of CD317 and Vpu between DRM and S fractions was determined by scanning Western blot membranes with the LI-COR imaging system that measures the infrared fluorescent signal emitted by the infrared dyes conjugated to secondary antibodies recognizing species-specific primary antibodies. Signals were quantified using the Odyssey software (Odyssey® Infrared Imaging System, Biosciences) following background subtraction. Each fraction was first individually quantified and the combined total signal from both fractions was then set to 100%. The value obtained for the individual DRM and S fraction for a given protein were then set relative to this 100%. For CD317 wt or CD317 KKAA, the combined signal for all individual CD317 species was taken into account as indicated by boxes. The quantification shown in Figs. 2, 3 and 7 represents the mean value of three independent DRM flotation assays, quantified as described, with the corresponding standard deviations.

Immunofluorescence microscopy

293T or TZM-bl cells growing on coverglasses or Jurkat Tag T cells adhered to poly-lysine coated coverglasses were fixed with 4% PFA and permeabilized for 2 min with 0.1% Triton X-100 in PBS. Cells were blocked for 1 h with 1% bovine serum albumin in PBS and stained with appropriate primary and secondary antibodies for detection of Vpu, HA, or CD317, respectively. Coverslips were mounted in mowiol and analyzed with a Zeiss LSM510 confocal microscope with a 100× PLAN-APO objective lens. Images were recorded with the Zeiss proprietary software LSM5 and processed with Adobe Photoshop 6.0.

Statistical evaluation

Statistical significance was determined using the paired Student's *t*-test.

Acknowledgments

This project is funded by the Deutsche Forschungsgemeinschaft (grant FA/378-11-1 to OTF and KE742/4-1 to OTK). We are grateful to Chugai Pharmaceuticals (mouse monoclonal anti-CD317 antibody), Stephen Robbins (expression constructs for Erlin and Flotilin), Klaus Strebel (rabbit anti-BST-2 antiserum) and Barbara Müller/Hans-Georg Kräusslich (anti-p24CA antibody) for generously providing reagents and to SFB638 for access to the LSM510 confocal microscope. O.T.F. and O.T.K. are members of the CellNetworks Cluster of Excellence EXC81.

References

Andrew, A.J., Miyagi, E., Strebel, K., 2011. Differential effects of human immunodeficiency virus type 1 Vpu on the stability of BST-2/Tetherin. J. Virol. 85, 2611–2619.
Banning, C., Votteler, J., Hoffmann, D., Koppensteiner, H., Warmer, M., Reimer, R., Kirchhoff, F., Schubert, U., Hauber, J., Schindler, M., 2010. A flow cytometry-based FRET assay to identify and analyse protein–protein interactions in living cells. PLoS One 5, e9344.
Browman, D.T., Resek, M.E., Zajchowski, L.D., Robbins, S.M., 2006. Erlin-1 and erlin-2 are novel members of the prohibitin family of proteins that define lipid-raft-like domains of the ER. J. Cell Sci. 119, 3149–3160.
Brown, D.A., Rose, J.K., 1992. Sorting of GPI-anchored proteins to glycolipid-enriched membrane subdomains during transport to the apical cell surface. Cell 68, 533–544.
Dube, M., Roy, B.B., Guiot-Guillain, P., Mercier, J., Binette, J., Leung, G., Cohen, E.A., 2009. Suppression of Tetherin-restricting activity upon human immunodeficiency virus type 1 particle release correlates with localization of Vpu in the trans-Golgi network. J. Virol. 83, 4574–4590.
Dube, M., Roy, B.B., Guiot-Guillain, P., Binette, J., Mercier, J., Chiasson, A., Cohen, E.A., 2010. Antagonism of Tetherin restriction of HIV-1 release by Vpu involves binding and sequestration of the restriction factor in a perinuclear compartment. PLoS Pathog. 6, e1000856.
Erikson, E., Adam, T., Schmidt, S., Lehmann-Koch, J., Over, B., Goffinet, C., Harter, C., Bekeredjian-Ding, I., Sertel, S., Lasitschka, F., Keppler, O.T., 2011. In vivo expression profile of the antiviral restriction factor and tumor-targeting antigen CD317/BST-2/HM1.24/Tetherin in humans. Proc. Natl. Acad. Sci. U. S. A. 108, 13688–13693.
Giese, S.I., Woerz, I., Homann, S., Tibroni, N., Geyer, M., Fackler, O.T., 2006. Specific and distinct determinants mediate membrane binding and lipid raft incorporation of HIV-1(SF2) Nef. Virology 355, 175–191.
Goffinet, C., Allespach, I., Homann, S., Tervo, H.M., Habermann, A., Rupp, D., Oberbremer, L., Kern, C., Tibroni, N., Welsch, S., Krijnse-Locker, J., Banting, G., Krausslich, H.G., Fackler, O.T., Keppler, O.T., 2009. HIV-1 antagonism of CD317 is species specific and involves Vpu-mediated proteasomal degradation of the restriction factor. Cell Host Microbe 5, 285–297.
Goffinet, C., Homann, S., Ambiel, I., Tibroni, N., Rupp, D., Keppler, O.T., Fackler, O.T., 2010. Antagonism of CD317 restriction of human immunodeficiency virus type 1 (HIV-1) particle release and depletion of CD317 are separable activities of HIV-1 Vpu. J. Virol. 84, 4089–4094.
Gupta, R.K., Hue, S., Schaller, T., Verschoor, E., Pillay, D., Towers, G.J., 2009. Mutation of a single residue renders human Tetherin resistant to HIV-1 Vpu-mediated depletion. PLoS Pathog. 5, e1000443.
Hauser, H., Lopez, L.A., Yang, S.J., Oldenburg, J.E., Exline, C.M., Guatelli, J.C., Cannon, P.M., 2010. HIV-1 Vpu and HIV-2 Env counteract BST-2/Tetherin by sequestration in a perinuclear compartment. Retrovirology 7, 51.
Hinz, A., Miguet, N., Natrajan, G., Usami, Y., Yamanaka, H., Renesto, P., Hartlieb, B., McCarthy, A.A., Simorre, J.P., Gottlinger, H., Weissenhorn, W., 2010. Structural basis of HIV-1 tethering to membranes by the BST-2/Tetherin ectodomain. Cell Host Microbe 7, 314–323.
Holm, K., Weclewicz, K., Hewson, R., Suomalainen, M., 2003. Human immunodeficiency virus type 1 assembly and lipid rafts: Pr55(gag) associates with membrane domains that are largely resistant to Brij98 but sensitive to Triton X-100. J. Virol. 77, 4805–4817.
Ishikawa, J., Kaisho, T., Tomizawa, H., Lee, B.O., Kobune, Y., Inazawa, J., Oritani, K., Itoh, M., Ochi, T., Ishihara, K., et al., 1995. Molecular cloning and chromosomal mapping of a bone marrow stromal cell surface gene, BST2, that may be involved in pre-B-cell growth. Genomics 26, 527–534.
Iwabu, Y., Fujita, H., Kinomoto, M., Kaneko, K., Ishizaka, Y., Tanaka, Y., Sata, T., Tokunaga, K., 2009. HIV-1 accessory protein Vpu internalizes cell-surface BST-2/Tetherin through transmembrane interactions leading to lysosomes. J. Biol. Chem. 284, 35060–35072.
Jouvenet, N., Neil, S.J., Zhadina, M., Zang, T., Kratovac, Z., Lee, Y., McNatt, M., Hatziioannou, T., Bieniasz, P.D., 2009. Broad-spectrum inhibition of retroviral and filoviral particle release by Tetherin. J. Virol. 83, 1837–1844.
Kaletsky, R.L., Francica, J.R., Agrawal-Gamse, C., Bates, P., 2009. Tetherin-mediated restriction of filovirus budding is antagonized by the Ebola glycoprotein. Proc. Natl. Acad. Sci. U. S. A. 106, 2886–2891.
Keppler, O.T., Allespach, I., Schuller, L., Fenard, D., Greene, W.C., Fackler, O.T., 2005. Rodent cells support key functions of the human immunodeficiency virus type 1 pathogenicity factor Nef. J. Virol. 79, 1655–1665.
Kobayashi, T., Ode, H., Yoshida, T., Sato, K., Gee, P., Yamamoto, S.P., Ebina, H., Strebel, K., Sato, H., Koyanagi, Y., 2011. Identification of amino acids in the human Tetherin transmembrane domain responsible for HIV-1 Vpu interaction and susceptibility. J. Virol. 85, 932–945.
Krautkramer, E., Giese, S.I., Gasteier, J.E., Muranyi, W., Fackler, O.T., 2004. Human immunodeficiency virus type 1 Nef activates p21-activated kinase *via* recruitment into lipid rafts. J. Virol. 78, 4085–4097.
Kuhl, B.D., Sloan, R.D., Donahue, D.A., Liang, C., Wainberg, M.A., 2011. Vpu-mediated Tetherin antagonism of ongoing HIV-1 infection in CD4(+) T-cells is not directly related to the extent of Tetherin cell surface downmodulation. Virology 417, 353–361.
Kupzig, S., Korolchuk, V., Rollason, R., Sugden, A., Wilde, A., Banting, G., 2003. Bst-2/HM1.24 is a raft-associated apical membrane protein with an unusual topology. Traffic 4, 694–709.
Lau, D., Kwan, W., Guatelli, J., 2011. Role of the endocytic pathway in the counteraction of BST-2 by human lentiviral pathogens. J. Virol. 85, 9834–9846.
Li, H., Papadopoulos, V., 1998. Peripheral-type benzodiazepine receptor function in cholesterol transport. Identification of a putative cholesterol recognition/interaction amino acid sequence and consensus pattern. Endocrinology 139, 4991–4997.

Li, N., Mak, A., Richards, D.P., Naber, C., Keller, B.O., Li, L., Shaw, A.R., 2003. Monocyte lipid rafts contain proteins implicated in vesicular trafficking and phagosome formation. Proteomics 3, 536–548.
Lindwasser, O.W., Resh, M.D., 2002. Myristoylation as a target for inhibiting HIV assembly: unsaturated fatty acids block viral budding. Proc. Natl. Acad. Sci. U. S. A. 99, 13037–13042.
Lingwood, D., Simons, K., 2010. Lipid rafts as a membrane-organizing principle. Science 327, 46–50.
Mangeat, B., Gers-Huber, G., Lehmann, M., Zufferey, M., Luban, J., Piguet, V., 2009. HIV-1 Vpu neutralizes the antiviral factor Tetherin/BST-2 by binding it and directing its beta-TrCP2-dependent degradation. PLoS Pathog. 5, e1000574.
Mansouri, M., Viswanathan, K., Douglas, J.L., Hines, J., Gustin, J., Moses, A.V., Fruh, K., 2009. Molecular mechanism of BST2/Tetherin downregulation by K5/MIR2 of Kaposi's sarcoma-associated herpesvirus. J. Virol. 83, 9672–9681.
Masuyama, N., Kuronita, T., Tanaka, R., Muto, T., Hirota, Y., Takigawa, A., Fujita, H., Aso, Y., Amano, J., Tanaka, Y., 2009. HM1.24 is internalized from lipid rafts by clathrin-mediated endocytosis through interaction with alpha-adaptin. J. Biol. Chem. 284, 15927–15941.
Michel, N., Allespach, I., Venzke, S., Fackler, O.T., Keppler, O.T., 2005. The Nef protein of human immunodeficiency virus establishes superinfection immunity by a dual strategy to downregulate cell-surface CCR5 and CD4. Curr. Biol. 15, 714–723.
Mitchell, R.S., Katsura, C., Skasko, M.A., Fitzpatrick, K., Lau, D., Ruiz, A., Stephens, E.B., Margottin-Goguet, F., Benarous, R., Guatelli, J.C., 2009. Vpu antagonizes BST-2-mediated restriction of HIV-1 release *via* beta-TrCP and endo-lysosomal trafficking. PLoS Pathog. 5, e1000450.
Miyagi, E., Andrew, A.J., Kao, S., Strebel, K., 2009. Vpu enhances HIV-1 virus release in the absence of Bst-2 cell surface down-modulation and intracellular depletion. Proc. Natl. Acad. Sci. U. S. A. 106, 2868–2873.
Morrow, I.C., Parton, R.G., 2005. Flotillins and the PHB domain protein family: rafts, worms and anaesthetics. Traffic 6, 725–740.
Neil, S.J., Zang, T., Bieniasz, P.D., 2008. Tetherin inhibits retrovirus release and is antagonized by HIV-1 Vpu. Nature 451, 425–430.
Nguyen, D.H., Hildreth, J.E., 2000. Evidence for budding of human immunodeficiency virus type 1 selectively from glycolipid-enriched membrane lipid rafts. J. Virol. 74, 3264–3272.
Nguyen, K.L., Llano, M., Akari, H., Miyagi, E., Poeschla, E.M., Strebel, K., Bour, S., 2004. Codon optimization of the HIV-1 vpu and vif genes stabilizes their mRNA and allows for highly efficient Rev-independent expression. Virology 319, 163–175.
Ono, A., Freed, E.O., 2001. Plasma membrane rafts play a critical role in HIV-1 assembly and release. Proc. Natl. Acad. Sci. U. S. A. 98, 13925–13930.
Pardieu, C., Vigan, R., Wilson, S.J., Calvi, A., Zang, T., Bieniasz, P., Kellam, P., Towers, G.J., Neil, S.J., 2010. The RING-CH ligase K5 antagonizes restriction of KSHV and HIV-1 particle release by mediating ubiquitin-dependent endosomal degradation of Tetherin. PLoS Pathog. 6, e1000843.
Perez-Caballero, D., Zang, T., Ebrahimi, A., McNatt, M.W., Gregory, D.A., Johnson, M.C., Bieniasz, P.D., 2009. Tetherin inhibits HIV-1 release by directly tethering virions to cells. Cell 139, 499–511.
Pfeiffer, T., Pisch, T., Devitt, G., Holtkotte, D., Bosch, V., 2006. Effects of signal peptide exchange on HIV-1 glycoprotein expression and viral infectivity in mammalian cells. FEBS Lett. 580, 3775–3778.
Radoshitzky, S.R., Dong, L., Chi, X., Clester, J.C., Retterer, C., Spurgers, K., Kuhn, J.H., Sandwick, S., Ruthel, G., Kota, K., Boltz, D., Warren, T., Kranzusch, P.J., Whelan, S.P., Bavari, S., 2010. Infectious Lassa virus, but not filoviruses, is restricted by BST-2/Tetherin. J. Virol. 84, 10569–10580.
Rauch, S., Pulkkinen, K., Saksela, K., Fackler, O.T., 2008. Human immunodeficiency virus type 1 Nef recruits the guanine exchange factor Vav1 *via* an unexpected interface into plasma membrane microdomains for association with p21-activated kinase 2 activity. J. Virol. 82, 2918–2929.
Rollason, R., Korolchuk, V., Hamilton, C., Schu, P., Banting, G., 2007. Clathrin-mediated endocytosis of a lipid-raft-associated protein is mediated through a dual tyrosine motif. J. Cell Sci. 120, 3850–3858.
Rong, L., Zhang, J., Lu, J., Pan, Q., Lorgeoux, R.P., Aloysius, C., Guo, F., Liu, S.L., Wainberg, M.A., Liang, C., 2009. The transmembrane domain of BST-2 determines its sensitivity to down-modulation by human immunodeficiency virus type 1 Vpu. J. Virol. 83, 7536–7546.
Ross, T.M., Oran, A.E., Cullen, B.R., 1999. Inhibition of HIV-1 progeny virion release by cell-surface CD4 is relieved by expression of the viral Nef protein. Curr. Biol. 9, 613–621.
Ruiz, A., Hill, M.S., Schmitt, K., Stephens, E.B., 2010. Membrane raft association of the Vpu protein of human immunodeficiency virus type 1 correlates with enhanced virus release. Virology 408, 89–102.
Sakuma, T., Noda, T., Urata, S., Kawaoka, Y., Yasuda, J., 2009. Inhibition of Lassa and Marburg virus production by Tetherin. J. Virol. 83, 2382–2385.
Schmidt, S., Fritz, J.V., Bitzegeio, J., Fackler, O.T., Keppler, O.T., 2011. HIV-1 Vpu blocks recycling and biosynthetic transport of the intrinsic immunity factor CD317/Tetherin to overcome the virion release restriction. mBio 2, e00036-11.
Serra-Moreno, R., Jia, B., Breed, M., Alvarez, X., Evans, D.T., 2011. Compensatory changes in the cytoplasmic tail of gp41 confer resistance to Tetherin/BST-2 in a pathogenic nef-deleted SIV. Cell Host Microbe 9, 46–57.
Simons, K., Ikonen, E., 1997. Functional rafts in cell membranes. Nature 387, 569–572.
Tervo, H.M., Homann, S., Ambiel, I., Fritz, J.V., Fackler, O.T., Keppler, O.T., 2011. beta-TrCP is dispensable for Vpu's ability to overcome the CD317/Tetherin-imposed restriction to HIV-1 release. Retrovirology 8, 9.
Van Damme, N., Goff, D., Katsura, C., Jorgenson, R.L., Mitchell, R., Johnson, M.C., Stephens, E.B., Guatelli, J., 2008. The interferon-induced protein BST-2 restricts HIV-1 release and is downregulated from the cell surface by the viral Vpu protein. Cell Host Microbe 3, 245–252.
Vigan, R., Neil, S.J., 2010. Determinants of Tetherin antagonism in the transmembrane domain of the human immunodeficiency virus type 1 Vpu protein. J. Virol. 84, 12958–12970.
Vishwanathan, S.A., Thomas, A., Brasseur, R., Epand, R.F., Hunter, E., Epand, R.M., 2008. Hydrophobic substitutions in the first residue of the CRAC segment of the gp41 protein of HIV. Biochemistry 47, 124–130.
Weidner, J.M., Jiang, D., Pan, X.B., Chang, J., Block, T.M., Guo, J.T., 2010. Interferon-induced cell membrane proteins, IFITM3 and Tetherin, inhibit vesicular stomatitis virus infection *via* distinct mechanisms. J. Virol. 84, 12646–12657.
Yang, H., Wang, J., Jia, X., McNatt, M.W., Zang, T., Pan, B., Meng, W., Wang, H.W., Bieniasz, P.D., Xiong, Y., 2010. Structural insight into the mechanisms of enveloped virus tethering by Tetherin. Proc. Natl. Acad. Sci. U. S. A. 107, 18428–18432.
Yondola, M.A., Fernandes, F., Belicha-Villanueva, A., Uccelini, M., Gao, Q., Carter, C., Palese, P., 2011. Budding capability of the influenza virus neuraminidase can be modulated by Tetherin. J. Virol. 85, 2480–2491.
Zheng, Y.Z., Foster, L.J., 2009. Biochemical and proteomic approaches for the study of membrane microdomains. J. Proteomics 72, 12–22.